

AD-A137 982

OBSERVATIONS OF VLF TRANSMITTER-INDUCED DEPLETIONS OF
INNER ZONE ELECTRON. (U) AEROSPACE CORP EL SEGUNDO CA
SPACE SCIENCES LAB A L VAMPOLA 09 DEC 83

1/1

UNCLASSIFIED

TR-0084(4940-05)-4 SD-TR-83-89

F/G 8/14

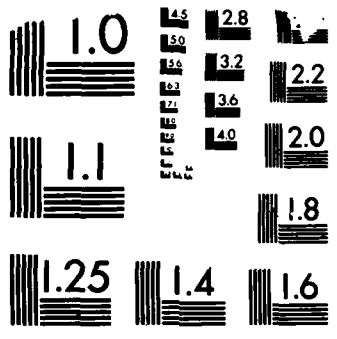
NL

END

FORM

83-

etc



MICROCOPY RESOLUTION TEST CHART
NATIONAL BUREAU OF STANDARDS-1963-A

12

ADA137982

Observations of VLF Transmitter-Induced Depletions of Inner Zone Electrons

A. L. VAMPOLA ✓
Space Sciences Laboratory
Laboratory Operations
The Aerospace Corporation
El Segundo, California 90245

9 December 1983

APPROVED FOR PUBLIC RELEASE;
DISTRIBUTION UNLIMITED

DTIC FILE COPY

Prepared for
SPACE DIVISION
AIR FORCE SYSTEMS COMMAND
Los Angeles Air Force Station
P.O. Box 9296), Worldway Postal Center
Los Angeles, California 90009

DTIC
FEB 17 1984
A

84 02 17 001

This report was submitted by The Aerospace Corporation, El Segundo, CA 90245, under Contract No. F04701-83-C-0084 with the Space Division, P.O. Box 92960, Worldway Postal Center, Los Angeles, CA 90009. It was reviewed and approved for The Aerospace Corporation by H. R. Ruge, Director, Space Sciences Laboratory. Captain Gary M. Rowe, SD/YCM, was the project officer for the Mission-Oriented Investigation and Experimentation (MOIE) program.

This report has been reviewed by the Public Affairs Office (PAS) and is releasable to the National Technical Information Service (NTIS). At NTIS, it will be available to the general public, including foreign nationals.

This technical report has been reviewed and is approved for publication. Publication of this report does not constitute Air Force approval of the report's findings or conclusions. It is published only for the exchange and stimulation of ideas.



Gary M. Rowe, Captain, USAF
Project Officer



Joseph Hess, GM-15, Director
West Coast Office, Air Force
Space Technology Center

UNCLASSIFIED

SECURITY CLASSIFICATION OF THIS PAGE (When Data Entered)

REPORT DOCUMENTATION PAGE		READ INSTRUCTIONS BEFORE COMPLETING FORM
1. REPORT NUMBER SD-TR-83-89	2. GOVT ACCESSION NO. AD-A137982	3. RECIPIENT'S CATALOG NUMBER
4. TITLE (and Subtitle) OBSERVATIONS OF VLF TRANSMITTER-INDUCED DEPLETIONS OF INNER ZONE ELECTRONS	5. TYPE OF REPORT & PERIOD COVERED	
	6. PERFORMING ORG. REPORT NUMBER TR-0084(4940-05)-4	
7. AUTHOR(s) A. L. Vampola	8. CONTRACT OR GRANT NUMBER(s) F04701-83-C-0084	
9. PERFORMING ORGANIZATION NAME AND ADDRESS The Aerospace Corporation El Segundo, California 90245	10. PROGRAM ELEMENT, PROJECT, TASK AREA & WORK UNIT NUMBERS	
11. CONTROLLING OFFICE NAME AND ADDRESS Space Division Los Angeles Air Force Station Los Angeles, California 90009	12. REPORT DATE 9 December 1983	
	13. NUMBER OF PAGES 20	
14. MONITORING AGENCY NAME & ADDRESS (if different from Controlling Office)	15. SECURITY CLASS. (of this report) Unclassified	
	15a. DECLASSIFICATION/DOWNGRADING SCHEDULE	
16. DISTRIBUTION STATEMENT (of this Report) Approved for public release; distribution unlimited.		
17. DISTRIBUTION STATEMENT (of the abstract entered in Block 20, if different from Report)		
18. SUPPLEMENTARY NOTES		
19. KEY WORDS (Continue on reverse side if necessary and identify by block number) Electron precipitation Wave-particle interaction Inner zone electrons		
20. ABSTRACT (Continue on reverse side if necessary and identify by block number) → Precipitation spikes of electrons, in which the energy spread of the peak is narrow (less than 50 keV) and the peak energy is a strong function of the location in L, have been observed in the region $1.5 < L < 2.0$ and have been ascribed to interactions between waves from high power VLF transmitters on the ground and the precipitated electrons. (Vampola and Kuck, 1978; Imhof et al., 1981). Instrumentation on the S3-2 satellite (polar orbit, 240 km and 1557 km perigee and apogee) included a large geometric factor electron		

DD FORM 1473
(FACSIMILE)UNCLASSIFIED
SECURITY CLASSIFICATION OF THIS PAGE (When Data Entered)

UNCLASSIFIED

SECURITY CLASSIFICATION OF THIS PAGE(When Data Entered)

19. KEY WORDS (Continued)

20. ABSTRACT (Continued)

spectrometer which, due to the characteristics of the instrument and orbit, routinely observed these precipitation spikes. Additionally, on numerous occasions when these spikes were observed at low altitude, a significant depletion of electrons at the same energies was observed high on the field line. These depletions indicate that the loss rate of electrons due to VLF transmitters is significant and usually exceeds the rate at which radial diffusion is refilling those field lines. Electrons with energies between 36 and 317 keV in the region $1.9 < L < 1.6$ were observed to have lifetimes limited to a few days by interactions with waves from VLF transmitters. Thus the outer edge of the inner zone is defined by this wave-particle process.

UNCLASSIFIED

SECURITY CLASSIFICATION OF THIS PAGE(When Data Entered)

CONTENTS

PREFACE.....	1
I. INTRODUCTION.....	7
II. DATA BASE.....	9
III. DATA.....	13
IV. DISCUSSION.....	21
REFERENCES.....	23

FIGURES

1.	D_{st} for the large magnetic storm on Day 86, 1976, and the period following.....	10
2.	S3-2 data for Day 86, 1976.....	12
3.	Data similar to Fig. 2 for Day 87, 1976.....	15
4.	Data similar to Fig. 2 for Day 90, 1976.....	16
5.	Data similar to Fig. 2 for Day 91, 1976.....	17
6.	Electron fluxes in the notch normalized to Day 87, 1976, data.....	18
7.	Effective electron lifetimes for the notches shown in Figs. 2 through 5.....	19

I. INTRODUCTION

The interaction of waves and particles in the magnetosphere is a topic of growing interest. One facet of the problem is the interaction between magnetospheric electrons and VLF waves from ground-based sources, principally high-powered VLF transmitters (Vampola and Kuck, 1978; Vampola, 1977; Koons et al., 1981; Imhof et al., 1981) and power-line harmonics (Helliwell et al., 1975). Vampola and Kuck (1978) used pitch-angle distributions of electrons in the drift loss cone to determine the longitude at which the electrons were precipitated into the loss cone [see Luhmann and Vampola (1977) for details of the tracing procedure]. The westernmost location coincided with the location of the high-power VLF transmitter, UMS, operating at a frequency of 16.2 kHz. The energy-vs-L dependence of the electron precipitation agreed with the assumption of a cyclotron interaction near the equator between the waves from the transmitter and the particles at the observed energy. Koons et al. (1981) extended the analysis of the data set by obtaining synoptic records of worldwide VLF transmissions and comparing them with the precipitation events. They were able to (1) determine which transmission periods from individual stations were responsible for particular electron precipitation events with specific energy structures, (2) identify two specific stations, UMS and NWC, as being responsible for inner zone electron precipitation, and (3) determine several of the interaction parameters under the assumption of a standard plasma density model. The calculations indicated a relatively low signal strength, 3 mV, was sufficient to precipitate the electrons. Such signal strengths are observed by satellites. Ray tracing techniques predicted an oblique interaction angle (61° with respect to the local field line) and an interaction within 15° of the magnetic equator. Imhof et al. (1981) presented the results of a similar study in which satellite measurements of precipitating electrons were compared with data from another satellite in which waves of the appropriate frequency were observed in the magnetosphere beyond the ionosphere.

In his paper, Vampola (1977) suggested that the interactions between man-made waves and electrons might be a significant factor in the development of the slot in the electron belts. In that scenario, the waves from the ground-based sources would interact with the electrons relatively low on the field line, producing an enlarged loss cone. The enlarged loss cone (and hence greater anisotropy in the distribution) would perhaps produce additional pitch-angle scattering of particles nearer the equator through an instability (Kennel and Petschek, 1966). The reason for specifying an interaction low on the field line (as opposed to the equatorial interaction utilized in the inner-zone analysis) was a requirement for frequency matching between the waves and the doppler-shifted cyclotron motion. Conditions could be met for the higher energy electrons only at relatively high B, hence low on the field line at the higher L value of the slot region.

Vampola (1977) also suggested that the inner zone electron environment might be even more severe than that observed following the Starfish enhancement were it not for the loss of these more energetic electrons as they undergo radial diffusion through the slot region. While we will not be able to test that hypothesis in this study, we will be able to address a related subject. In this report, we will examine the relative rates of pitch-angle diffusion versus radial diffusion for electrons in the interval $2 > L > 1.5$. The result is that pitch-angle diffusion lifetimes due to interactions with the VLF waves are much shorter than the radial diffusion rate. Thus, the outer edge of the inner zone is controlled by, and is probably the result of, interactions with waves from ground-based VLF transmitters.

II. DATA BASE

The data base being used in this study comes from a magnetic electron spectrometer on the USAF Space Test Program S3-2 satellite. The S3-2 was a relatively low altitude vehicle, 240 to 1557 km altitude, polar orbiting and spin-stabilized, with the spin vector nominally perpendicular to the orbit plane. Instruments viewed normal to the spin vector. Thus, complete pitch-angle distributions which included the local loss cones were usually obtained. For the L region of interest, the data were obtained reasonably close to the equator where the interactions between the waves and the electrons presumably are occurring. Values of B/B_0 for the location of observation varied from about 1.4 to 3, with the higher values at higher L. The data are, however, quite suitable for addressing the question of pitch-angle versus radial diffusion (i.e., stable trapping lifetimes). This is probably the first time that data have been presented that show the erosion of electron fluxes in the inner zone due to these wave-particle interactions. (For a change, we are showing and studying the hole instead of the material from the hole!)

For the purposes of this report, we will be using data obtained immediately after a major magnetic storm which occurred on 26 March 1976. Beall et al. (1967) showed that large fluxes of low energy electrons, < 0.5 MeV, are added to the inner zone by large magnetic storms. Electrons of higher energy are also added, but fluxes are much smaller and more difficult to detect (Vampola, 1972). During such large storms, the radial diffusion rate is much enhanced and electrons survive traversal through the slot region. The storm of 26 March 1976 presents us with a new population of electrons which we may observe until a second storm on 1 April 1976 again adds a large new population. Storms as large as these are rare, occurring at an average rate of once or twice per year over a solar cycle. Figure 1 is a plot of D_{st} at 8-hour intervals. The double arrow denotes the times of data shown on Figure 2. Arrows at later times show periods represented by the data of Figures 3 through 6. After the second storm (denoted Day 92 on Figure 1),

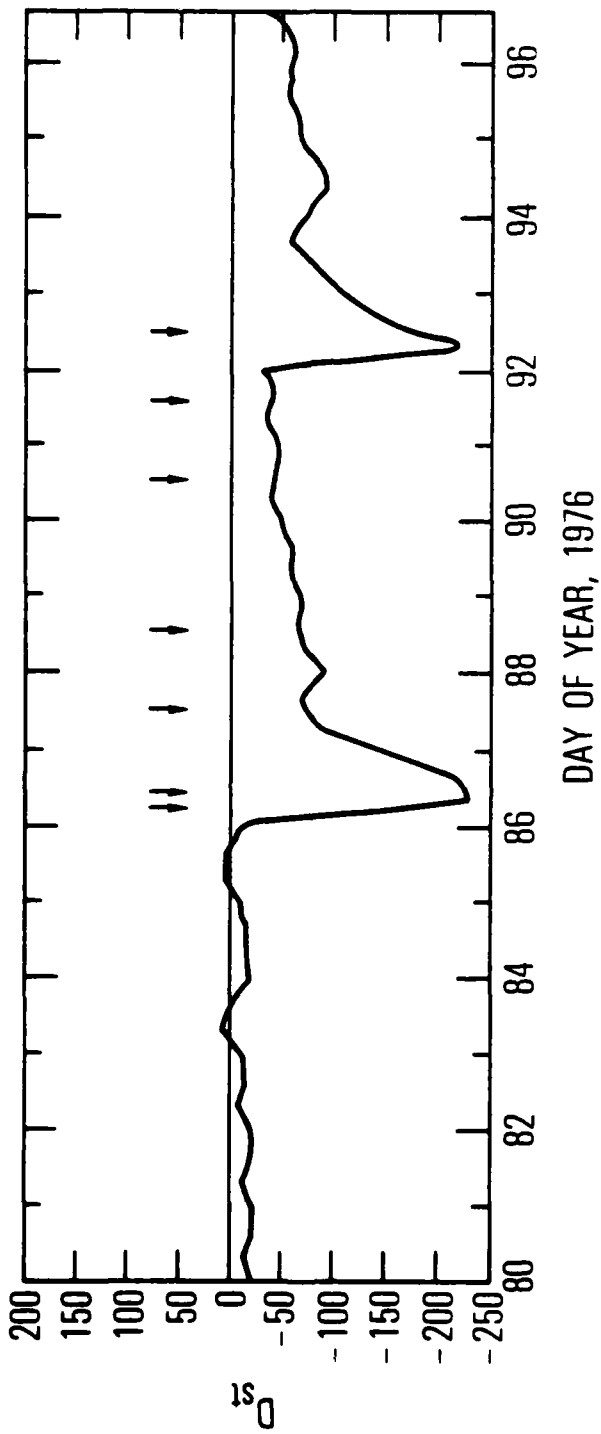
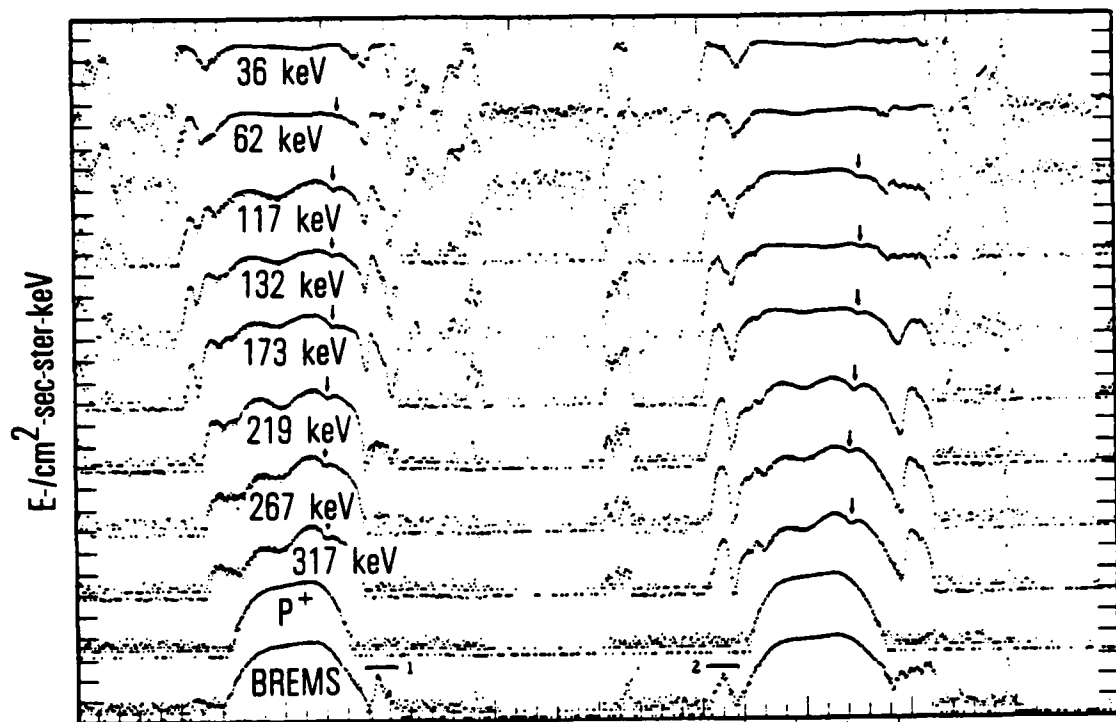


Fig. 1. Dst for the large magnetic storm on Day 86, 1976, and the period following. The arrows represent times of magnetic storm onset in the anomaly region were available from S3-2

large fluxes of electrons are added to the inner zone and the sequence of plots is terminated.

Since data relatively near the equator are required for this study, data were selected in the range of longitudes between 290° East Longitude and 25° East Longitude since in that region the S3-2 apogee is in the stable trapping region for values of L up to about 1.9. Figure 2 presents time plots of data for all of the S3-2 magnetic electron spectrometer data channels--eight electron channels plus two background channels. Data were plotted only when the pitch-angle was between 80° and 100°, i.e., J_{perp} data. The vertical scale is logarithmic, with tick marks being one decade. Data channels are offset by three decades for clarity. Count-rates are presented for the two background channels and fluxes for the electron channels. The lowest trace is from the "bremsstrahlung" channel. This channel is sensitive to electrons greater than 5 MeV (which penetrate through the walls of the satellite and the chamber of the spectrometer) and to energetic protons (>60 MeV) which are "corner-cutters" (such that the path-length through the detector is less than about 2/3 of the thickness of the detector). The second trace from the bottom, labeled "P⁺", counts the penetrating protons which pass completely through the detector. About 96% of these penetrating protons are counted in this channel with the remaining 4% being the "corner-cutters" mentioned above. Counts in these two channels normally indicate that the vehicle is in the stable trapping region of the magnetosphere, since the lifetime of the energetic protons is very long and replenishment is very slow. Thus, counts in the proton channel show the vehicle is in the stable trapping region. The eight traces above the background channels are electron channels. For these, energy decreases toward the top of the plot. The range of the centroids of response of the differential energy channels varies from 317 keV down to 36 keV.



UT	27698	28299	28639	33645	34245	34845	35447
B	0.2453	0.1772	0.1921	0.2520	0.1743	0.1715	0.2115
L	1.70	1.20	1.62	2.09	1.25	1.45	2.42
ELNG	42.1	35.5	29.5	18.2	11.2	5.3	357.5
LAT	38.1	8.5	-22.1	44.1	14.5	-15.8	-48.1

Fig. 2. S3-2 data for Day 86, 1976. The data are J_{perp} for two consecutive passes through the stable trapping region of the inner zone. The top 8 traces are electron fluxes, the ninth is a proton background monitor, and the tenth is a bremsstrahlung monitor. The arrows indicate an energy-dependent notch in the electron fluxes.

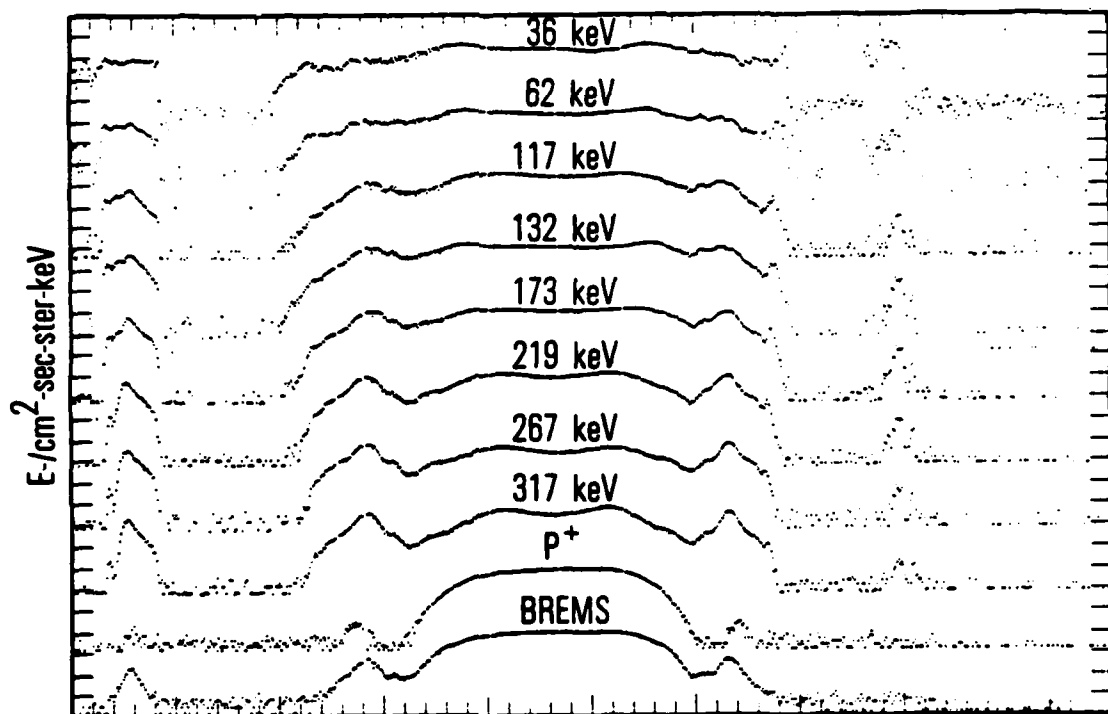
III. DATA

In Figure 2, the "bremsstrahlung" channel exhibits a normal response for the two passes through the stable trapping region defined by the P^+ monitor. The first of these passes occurs during the peak (in D_{st}) of the storm. The bar labeled "1" indicates a set of high-energy electrons which were accelerated by a previous storm and are diffusing radially to the inner zone. The time-constant for diffusion for these very energetic electrons is relatively long ($\approx 10^{-3}$ L/Day). Note that there is a strong altitude dependence on this structure. At the same L shell on the other side of the equator, the satellite is at lower altitude and the structure is barely visible. The arrows on the electron profiles on this pass show an L-dependent depletion (lower L for higher energies) which could be the result of the wave-particle interactions we have been discussing or a transient notch where freshly injected/accelerated electrons are merging into the slope of the outer edge of the inner zone and are not as high in intensity. The next pass, shown at later time on this same plot, occurs after the onset of the storm (see Figure 1). The storm precipitates large fluxes of electrons at all energies. The bar labeled "2" shows this precipitation at an altitude similar to the previous pass where there were essentially no electrons observed. In the previous pass, the electron channels showed strong erosion of the fluxes over a wide L range at low altitude (northern latitude pass). In the second pass, there has been significant filling of the low-altitude portion of the field lines, but there is evidence that wave-particle interactions have been removing electrons from selected regions of L. The profile is probably due primarily to the fact that the fluxes had been depleted at higher altitudes and pitch-angle scattering is strongly enhanced over all L intervals and energies, thus providing a low-altitude profile similar to the high altitude profile. The arrows on the second pass show that at high altitude there is no significant change, yet, in the inner zone. However, this second pass does show a strong addition of energetic particles in the slot region.

Figure 3, the next day, presents smooth profiles throughout the inner zone for all energies and also shows a significant filling of the slot region. Superposition of Figure 3 and a similar plot from the following day (not shown because of lack of space) shows the inner edge of the outer zone has migrated slightly to lower L, but otherwise relatively little change has occurred. Certainly no significant erosion has occurred in the inner zone. This indicates that for this period at least, either the wave-particle interactions were not occurring or the rate of radial diffusion was fast compared to the rate of pitch-angle diffusion. Figure 4 shows a different result. By Day 90, energy-dependent precipitation spikes are visible at the start of the plot at energies below 173 keV. The arrows show an L-dependent notch at energies below 219 keV. Figure 5 shows a continuation of the erosion process. On Day 92 (not shown, but see Figure 6), the notches are again partially filled. For these data, the radial-diffusive effects are clearly far stronger than the pitch-angle diffusive effects due to interactions with ground-based transmitters. However, storms which add electrons to the inner zone are relatively rare while the wave-particle interactions occur most of the time. Thus, as shown by Figures 2 through 5, the ground-based transmitters do have a pronounced effect on the inner zone morphology--they effectively change the lifetime of particles in a selected range of L values.

Figure 6 shows the reduction in flux intensity for each energy as a function of time after the storm. Data were normalized to the replenished profile in Figure 3. The small numeral indicates the channel number, with "1" being 36 keV and "8" being 317 keV. The general trend is for the high energy electrons to be less replenished immediately after the storm and for the loss rate of the lower energy electrons to be greater. Since the actual loss rate for any given time period depends upon a complex set of conditions (VLF transmitter activity, plasmaspheric conditions as a function of local time, etc.), one probably cannot make any inferences about the lack of monotonicity in the energy response.

Using the data of Figure 6, one obtains the effective lifetimes shown in Figure 7. The two points for each energy represent the lower and the upper lifetimes determined from the data. Since a very short period of time such as



UT	45338	45640	45942	46243	46544	46846	47147
B	0.2515	0.2114	0.1748	0.1517	0.1489	0.1707	0.2288
L	2.46	1.69	1.38	1.28	1.31	1.48	1.93
ELONG	328.8	324.8	321.7	318.8	315.7	312.1	307.1
LAT	40.7	25.9	10.9	-4.9	-19.8	-36.0	-52.9

Fig. 3. Data similar to Fig. 2 for Day 87, 1976. The energy-dependent notch has disappeared. Detail in the slot region (outside the stable trapping region shown by the proton monitor) is due to heavy precipitation in the slot region.

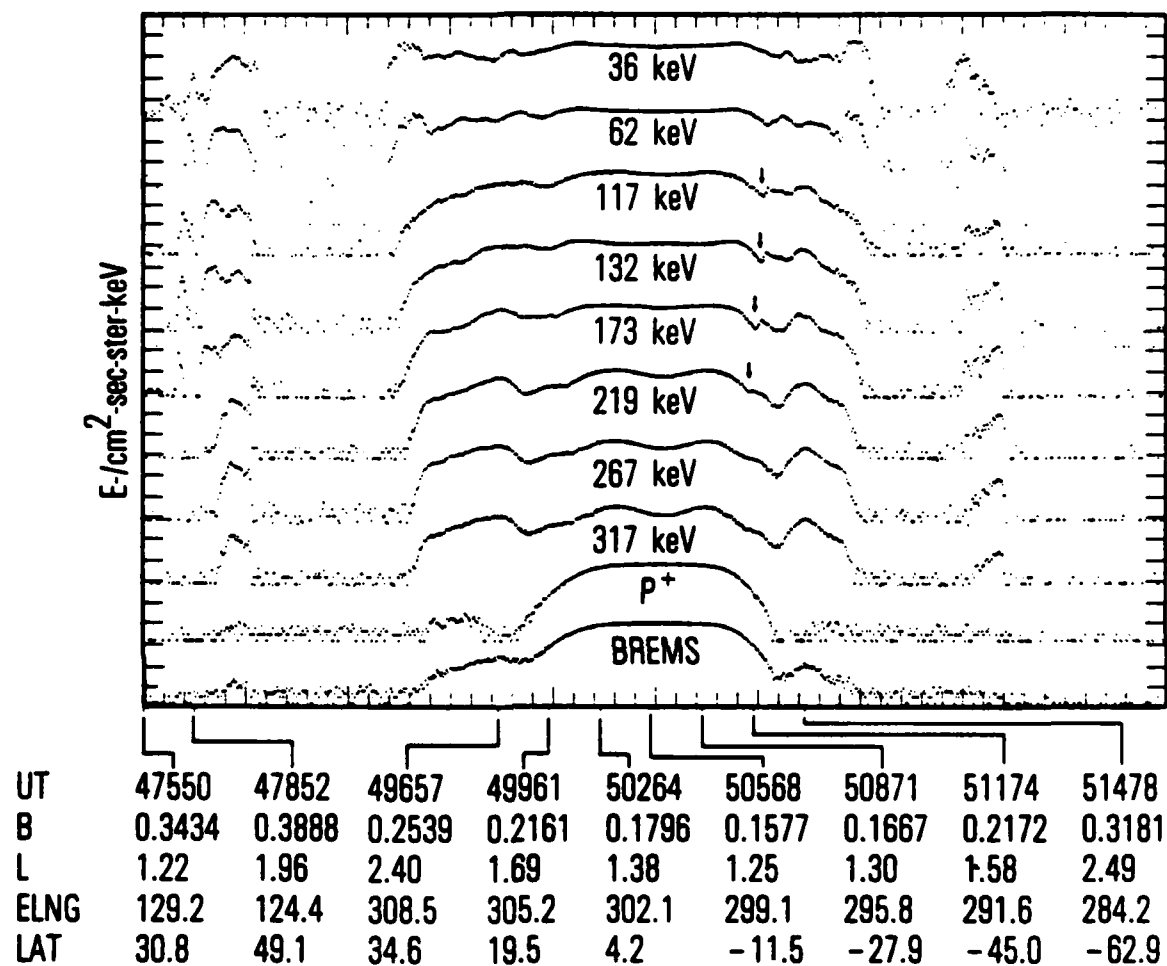


Fig. 4. Data similar to Fig. 2 for Day 90, 1976. Note that the energy-dependent notch has reappeared.

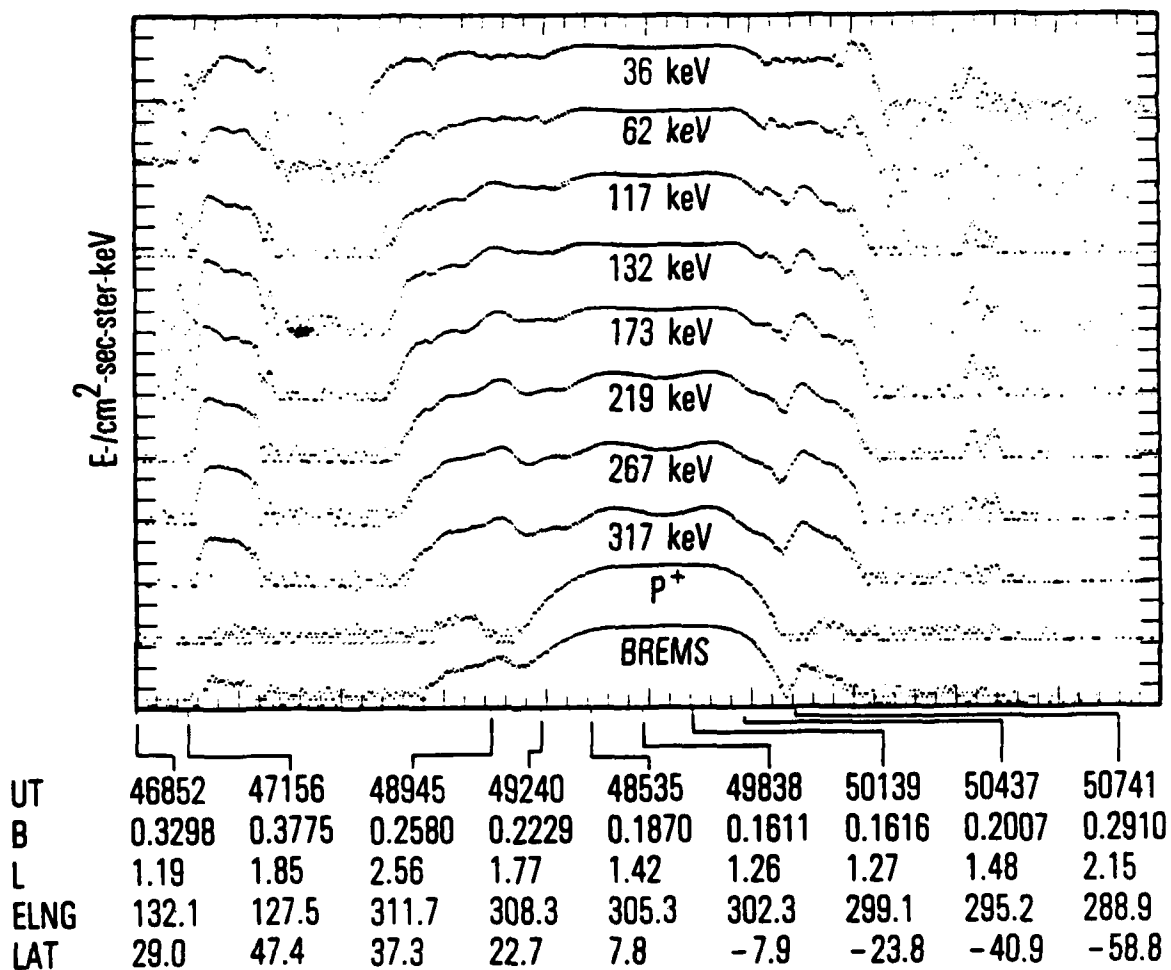


Fig. 5. Data similar to Fig. 2 for Day 91, 1976. The energy-dependent notch is deeper, and fluxes at slightly higher L values are significantly eroded, even though they are within the stable trapping region shown by the proton monitor.

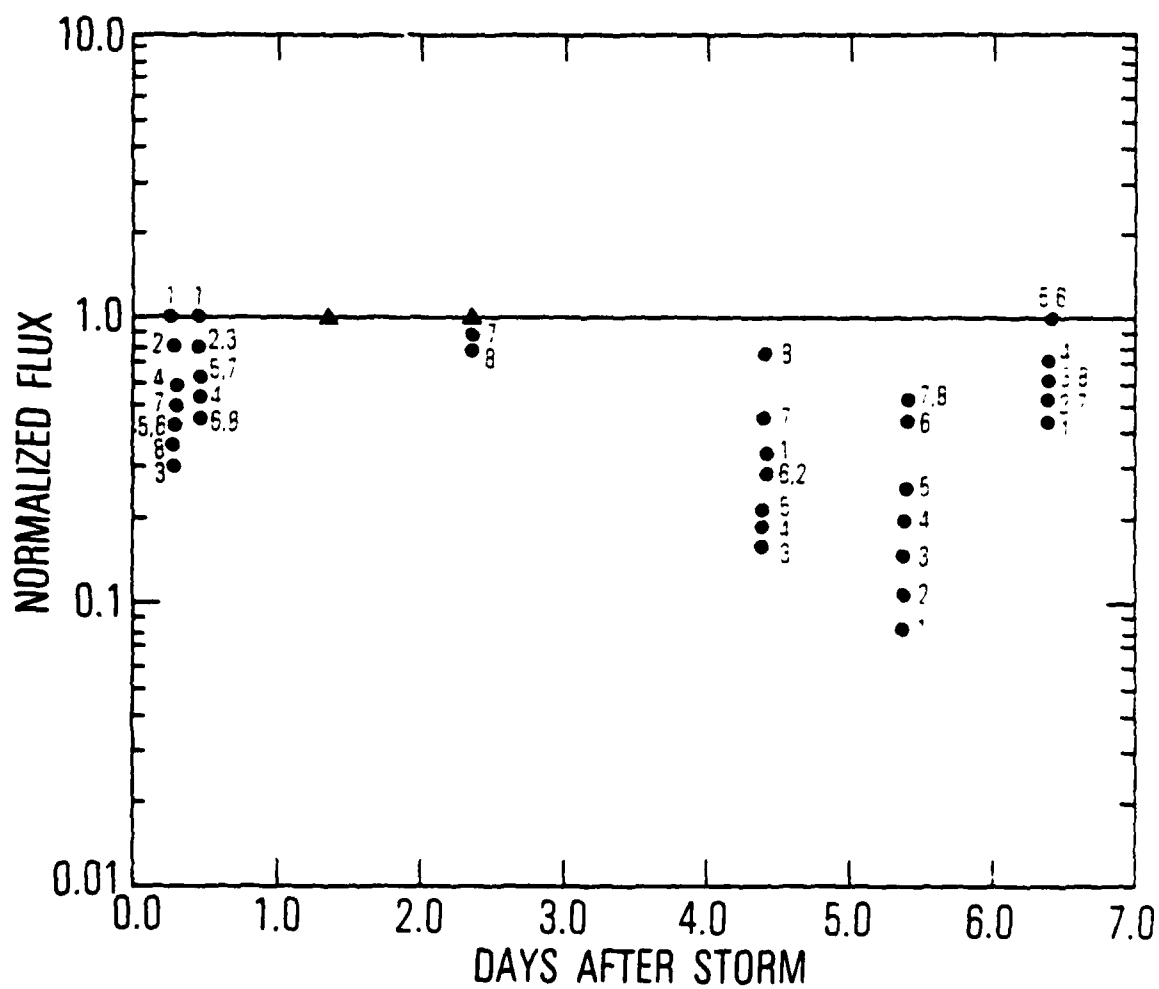


Fig. 6. Electron fluxes in the notch normalized to Day 87, 1976, data. Numerals indicate energy channel, with "1" being 36 keV and "8" being 317 keV.

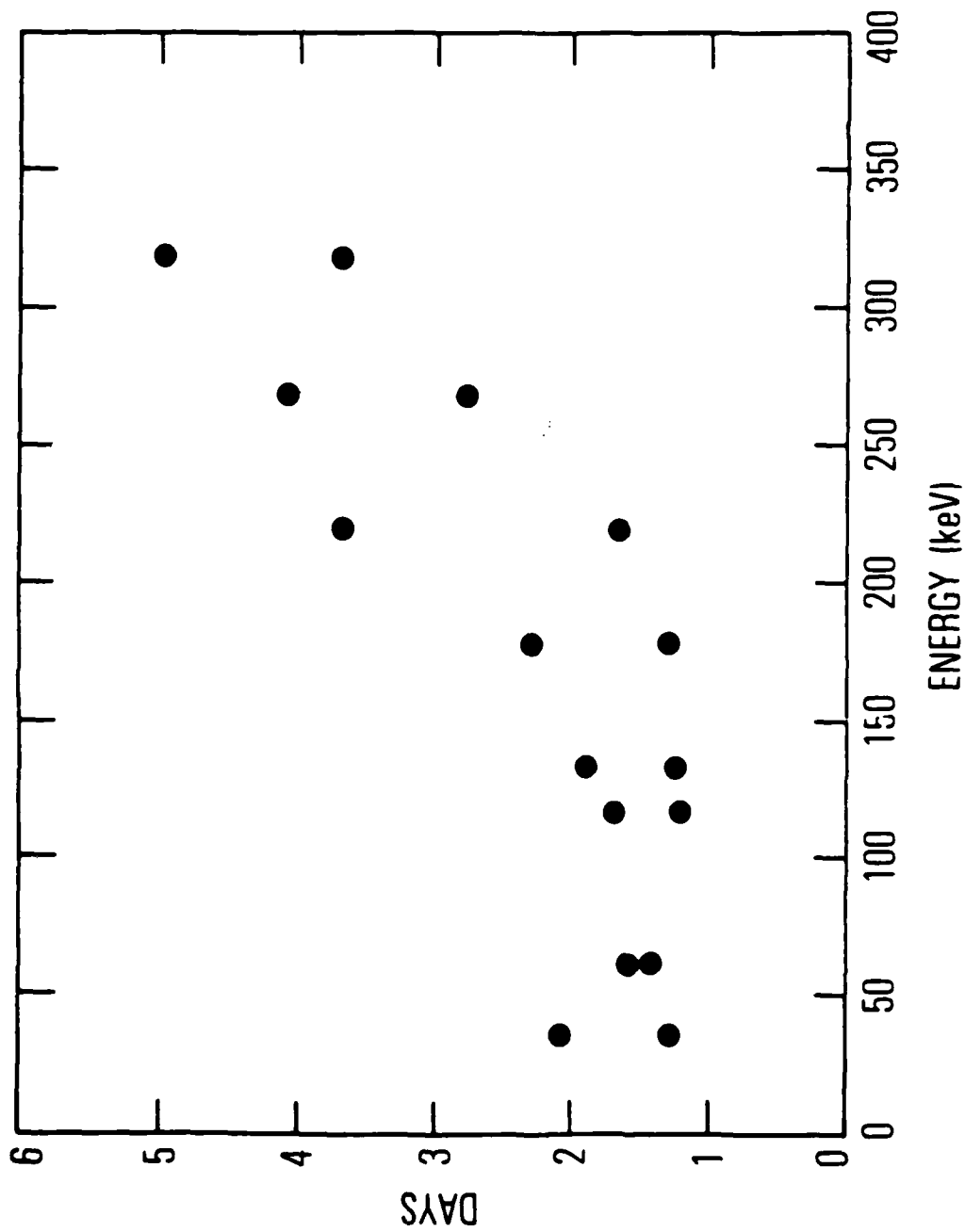


Fig. 7. Effective electron lifetimes for the notches shown in Figs. 2 through 5. Data are derived from Fig. 6.

the one used in this analysis may not be representative of the average conditions, these lower and upper limits may not bracket the long-term average lifetime. However, they can be used as an indication of the order of the magnitude of the lifetime of electrons in this energy range under the influence of VLF-wave pitch-angle scattering. Note that the lifetime measured here is a net lifetime, with particles being added by radial diffusion which partially compensate for the particles which are lost through pitch-angle scattering.

IV. DISCUSSION

The flux variations shown in Figures 2 through 6 show that pitch angle diffusion rates due to ground-based VLF transmitters (identified by the energy-dependent notch) exceed the radial diffusion rate in the outer edge of the inner zone. Figure 7 shows the limits to the pitch-angle diffusion lifetime for this time period. By observing the range in L over which pitch-angle scattering by VLF transmitters occurs, one can evaluate the total loss rate as electrons diffuse through this "hazard" region into the inner zone. The width of this region at a given energy can be determined either by using a single event or by using the spread in L of various events at a given peak energy [Figures 3 and 9, respectively, from Vampola and Kuck (1978)]. In either case, the result is the same; an electron must diffuse about 0.15 to 0.2 L during which time it is subject to pitch angle scattering by a given transmitter.

Radial diffusion rates for electrons in the inner zone during magnetically quiet periods are of the order of 10^{-4} to 10^{-5} L/Day for the region $1.9 < L < 1.5$ (Tomassian et al., 1972). Hence, it takes these electrons tens to hundreds of days to diffuse across the L region over which they are subject to precipitation by VLF stations. Thus, it appears that electrons can get into the inner zone only during periods when radial diffusion is much enhanced, i.e., during magnetic storm periods.

One final consideration is the question of lifetime due to pitch-angle scattering by VLF waves from transmitters compared to the lifetime against scattering by naturally occurring waves. Lyons et al. (1972) calculate lifetimes of hundreds of days for electrons in the energy and L range of this investigation. Since the effect of the VLF transmitters is to reduce the lifetime of the electrons to a small fraction of the radial diffusion time-constant and the artificially-induced lifetime is short compared to calculated natural pitch-angle lifetimes, the inevitable conclusion is that the VLF transmitters control the shape of the outer edge of the inner zone, in fact cause it, and prevent a large build-up of electrons in the inner zone. As was

pointed out by Vampola (1977), no measurements of magnetospheric particles previous to the construction of high-powered VLF transmitters exist.

That paper also pointed out that precipitation data in the slot region are inconsistent with the mechanism of Lyons et al. (1972) and may be entirely due to other ground-based VLF transmitters. That paper, together with the present results, indicates that the entire slot region may be an artifact of man's activities. If satellites replace VLF transmitters for both communication and navigation, we may have a chance to observe the slot refill and remain filled. If that happens, we will also see the inner zone become a very enhanced region, perhaps more enhanced even than during the post-Starfish period. We might have to continue to radiate VLF waves at high power levels in order to protect low altitude satellites.

REFERENCES

1. Beall, D. S., C. O. Bostrom, and D. J. Williams, "Structure and Decay of the Starfish Radiation Belt, October 1963 to December 1965," *J. Geophys. Res.*, 72, 3404 (1967).
2. Helliwell, R. A., J. P. Katsufakis, T. F. Bell, and R. Raghuram, "VLF Line Radiation in the Earth's Magnetosphere and Its Association with Power System Radiation," *J. Geophys. Res.*, 80, 4249 (1975).
3. Imhof, W. L., R. R. Anderson, J. B. Reagan, and E. E. Gains, "The Significance of VLF Transmitters in the Precipitation of Inner Belt Electrons," *J. Geophys. Res.*, 86, 11225 (1981).
4. Kennel, C. F. and H. E. Petschek, "Limit on Stably Trapped Particles," *J. Geophys. Res.*, 71, 1 (1966).
5. Koons, H. C., B. C. Edgar, and A. L. Vampola, "Precipitation of Inner Zone Electrons by Whistler Mode Waves from the VLF Transmitters UMS and NWC," *J. Geophys. Res.*, 86, 640 (1981).
6. Luhmann, J. G. and A. L. Vampola, "Effects of Localized Sources on Quiet-Time Plasmasphere Electron Precipitation," *J. Geophys. Res.*, 82, 2671 (1977).
7. Lyons, L. R., R. M. Thorne, and C. F. Kennel, "Pitch-Angle Diffusion of Radiation Belt Electrons Within the Plasmasphere," *J. Geophys. Res.*, 77, 3455 (1972).
8. Tomassian, A. D., T. A. Farley, and A. L. Vampola, "Inner Zone Energetic Electron Repopulation by Radial Diffusion," *J. Geophys. Res.*, 77, 3441 (1972).
9. Vampola, A. L., "Natural Variations in the Geomagnetically Trapped Electron Population," in Proceedings of the National Symposium on Natural and Manmade Radiations in Space, NASA TM X-2440, edited by E. A. Warman, p. 539 (1972).
10. Vampola, A. L., "VLF Transmission Induced Slot Electron Precipitation," *Geophys. Res. Lett.*, 4, 569 (1977).
11. Vampola, A. L. and G. A. Kuck, "Induced Precipitation of Inner Zone Electrons 1. Observations," *J. Geophys. Res.*, 83, 2543 (1978).

LABORATORY OPERATIONS

The Laboratory Operations of The Aerospace Corporation is conducting experimental and theoretical investigation, necessary for the evaluation and application of scientific advances to new military space systems. Versatility and flexibility have been developed to a high degree by the laboratory personnel in dealing with the many problems encountered in the nation's rapidly developing space systems. Expertise in the latest scientific developments is vital to the accomplishment of tasks related to these problems. The laboratories that contribute to this research are:

Aerophysics Laboratory: Launch vehicle and reentry aerodynamics and heat transfer, propulsion chemistry and fluid mechanics, structural mechanics, flight dynamics; high-temperature thermomechanics, gas kinetics and radiation; research in environmental chemistry and contamination; cw and pulsed chemical laser development including chemical kinetics, spectroscopy, optical resonators and beam pointing, atmospheric propagation, laser effects and countermeasures.

Chemistry and Physics Laboratory: Atmospheric chemical reactions, atmospheric optics, light scattering, state-specific chemical reactions and radiation transport in rocket plumes, applied laser spectroscopy, laser chemistry, battery electrochemistry, space vacuum and radiation effects on materials, lubrication and surface phenomena, thermionic emission, photosensitive materials and detectors, atomic frequency standards, and bioenvironmental research and monitoring.

Electronics Research Laboratory: Microelectronics, GaAs low-noise and power devices, semiconductor lasers, electromagnetic and optical propagation phenomena, quantum electronics, laser communications, lidar, and electro-optics; communication sciences, applied electronics, semiconductor crystal and device physics, radiometric imaging; millimeter-wave and microwave technology.

Information Sciences Research Office: Program verification, program translation, performance-sensitive system design, distributed architectures for spaceborne computers, fault-tolerant computer systems, artificial intelligence, and microelectronics applications.

Materials Sciences Laboratory: Development of new materials: metal matrix composites, polymers, and new forms of carbon; component failure analysis and reliability; fracture mechanics and stress corrosion; evaluation of materials in space environment; materials performance in space transportation systems; analysis of systems vulnerability and survivability in enemy-induced environments.

Space Sciences Laboratory: Atmospheric and ionospheric physics, radiation from the atmosphere, density and composition of the upper atmosphere, aurorae and airglow; magnetospheric physics, cosmic rays, generation and propagation of plasma waves in the magnetosphere; solar physics, infrared astronomy; the effects of nuclear explosions, magnetic storms, and solar activity on the earth's atmosphere, ionosphere, and magnetosphere; the effects of optical, electromagnetic, and particulate radiations in space on space systems.

. . .

FILM
4-8